



HAL
open science

Bacteria-Based Production of Thiol-Clickable, Genetically Encoded Lipid Nanovesicles

Jorge Royes, Oana Iliaia, Quentin Lubart, Federica Angius, Galina V
Dubacheva, Marta Bally, Bruno Miroux, Christophe C. Tribet

► **To cite this version:**

Jorge Royes, Oana Iliaia, Quentin Lubart, Federica Angius, Galina V Dubacheva, et al.. Bacteria-Based Production of Thiol-Clickable, Genetically Encoded Lipid Nanovesicles. *Angewandte Chemie*, 2019, 131 (22), pp.7473-7477. 10.1002/ange.201902929 . hal-02308493

HAL Id: hal-02308493

<https://hal.science/hal-02308493>

Submitted on 8 Oct 2019

HAL is a multi-disciplinary open access archive for the deposit and dissemination of scientific research documents, whether they are published or not. The documents may come from teaching and research institutions in France or abroad, or from public or private research centers.

L'archive ouverte pluridisciplinaire **HAL**, est destinée au dépôt et à la diffusion de documents scientifiques de niveau recherche, publiés ou non, émanant des établissements d'enseignement et de recherche français ou étrangers, des laboratoires publics ou privés.

Bacterial-based production of Thiol *Clickable* Genetically Encoded Lipid Nanovesicles

Jorge Royes,^[a,b] Oana Illoaia,^[b] Quentin Lubart,^[c] Federica Angius,^[b] Galina V. Dubacheva,^[c] Marta Bally,^[c] Bruno Miroux,^{*[b]} Christophe Tribet^{*[a]}

Abstract: Despite growing research efforts on the preparation of (bio)functional liposomes, synthetic capsules cannot reach the densities of protein loading and the control over peptide display that is achieved by natural vesicles. Here we present a microbial platform for high yield production of lipidic nanovesicles, with *clickable* thiol moieties in their outer corona. These nanovesicles show low size dispersity, are decorated with a dense, perfectly oriented and customizable corona of transmembrane polypeptides. In addition, this approach enables encapsulation of soluble proteins into the nanovesicles. Due to the mild preparation and loading conditions (absence of organic solvents, pH gradients or detergents) and their straightforward surface functionalization taking advantage of the diversity of commercially-available maleimide derivatives, engineering bacterial-based proteoliposomes are an attractive eco-friendly alternative that can outperform current liposome preparation methods.

Microbial biosynthesis offers significant advantages when *in glassware* synthesis is cost-intensive and/or provides poor yield and is particularly relevant for the preparation of fragile biomolecules.^[1] Nowadays it is no longer limited to small molecules. With a growing demand for renewable sources and sustainable industrial processes, bioproduction can be an eco-friendly response for the preparation more advanced materials, such as polymers,^[2] metal oxide nanoparticles^[3,4] and supramolecular assemblies of proteins.^[5,6]

To our knowledge, bioproduction has hardly been considered as an alternative to *in glassware* synthesis for lipidic nanovesicles, though membranes and compartments are ubiquitous in cells. This contrasts with the variety of applications of synthetic liposomes, used as encapsulation systems in consumer products^[7] and nano-medicine to protect fragile active compounds.^[8] Synthetic liposomes are advantageously

displaying a variety of molecules on their outer coronae, including polymers, peptides, fluorophores, etc, which is key to achieve optimal shelf-life, targeting, imaging functions. Accordingly, post-modifications in the corona of biological proteoliposomes (by conjugation with functional groups) is needed to approach the state of art of artificial lipid capsules. A recent renewal in this field came from nanovesicles secreted by cells in various physiological and pathological conditions.^[9] Such extracellular vesicles hold promises on innovative therapies and diagnostics, but their recovery from cell extracts and batch-to-batch reproducibility are poor.^[10,11] The interest for extracellular vesicles is an additional motivation for a versatile bioproduction of proteoliposomes. To obtain artificial proteoliposomes and/or mimics of membrane cells, the common (*in vitro*) route is to reconstitute purified membrane proteins into liposomes form detergent solutions.^[12,13] The quality of insertion of membrane proteins (native folding and control over in/out orientation) and protein densities are however far from approaching the natural, cell-secreted vesicles.^[11] Due their easy manipulation, bacteria provide the most affordable and handy source for nanovesicle bioproduction.^[14] Diverting the lipid synthesis and protein insertion cellular machineries may unlock the access towards more controlled proteoliposomes, providing a versatile, eco-friendly source of functional lipid:protein capsules.

We present here a platform for the production of bacterial-sourced proteoliposomes. We obtained well-defined, protein-loaded nanovesicles displaying a high density surface *clickable* groups (thiols from cysteine-containing tags). At variance with previously described approaches, it does not rely on outer membrane vesicle secretion suffering from low rate of vesiculation.^[15] In contrast, we triggered the proliferation of internal membranes to increase the vesicle yield,^[16,17] producing at the same time a dense array of engineered proteins on the nanovesicle surface. Internal membrane proliferation was achieved by overproducing an engineered membrane protein derived from AtpF, the b subunit of F₀F₁ ATP synthase (ATP-b), in C43(DE3) *E. coli* strain. This strain specifically evolved and trained to produce and fold ATP-b at high levels.^[17,18] Up to now, they were never considered as a tool to prepare and functionalize proteoliposomes. To this aim, we constructed a chimeric membrane protein, derived from AtpF, the b subunit of F₀F₁ ATP synthase (ATP-b).^[17] We characterized the composition, lipid:protein ratio and explored the surface functionalization (*via* thiol-maleimide *click chemistry*) of the bioproduced vesicles (Figure 1).

Nanovesicle production, isolation and composition analysis

The membrane proliferation induced by ATP-b overproduction in C43 (DE3) *E. coli* strain was the chassis for the preparation of lipidic nanovesicles containing custom polypeptides (Figure 1a). Overproduction of the unmodified *wild type* ATP-b was compared to ATP-b functionalized with a FIAsh tag and a Tobacco Etch Virus protease (TEV) digestion sequences (quoted ATP-b/F/T) both inserted at position 35,^[17] immediately after the membrane interaction domain (Figure 1c and Figure S1 in Supporting Info. N.B.: Attempts to produce ATP-b C-ter and N-ter fusion proteins failed to induce membrane proliferation and conducted to protein inclusion bodies).^[19] FIAsh tag enables in

[a] Dr. J. Royes, Dr. C. Tribet*
PASTEUR, Département de Chimie
École Normale Supérieure, PSL University, Sorbonne Université,
CNRS

24 rue Lhomond, 75005 Paris France

E-mail: christophe.tribet@ens.fr

[b] Dr. J. Royes, Mrs. O. Illoaia, Dr. F. Angius, Dr. B. Miroux*
UMR7099, Institut de Biologie Physico-Chimique, CNRS, Univ.

Paris Diderot, Sorbonne Université

13 rue Pierre et Marie Curie, 75005 Paris, France

Email: bruno.miroux@ibpc.fr

[c] Dr. Q. Lubart, Dr. M. Bally
Department of Physics, Chalmers University of Technology,
Gothenburg, Sweden.

[d] Dr. G. V. Dubacheva
PPSM, CNRS, École Normale Supérieure Paris-Saclay, Université
Paris-Saclay

61 Avenue du Président Wilson, 94235 Cachan, France

situ specific fluorescence labeling,^[20] allowing to identify and characterize the recombinant protein (Figure 1b). Additionally, its tetra-cysteine motif offers a mean for *in vitro* post-modifications via thiol-maleimide *click chemistry*.

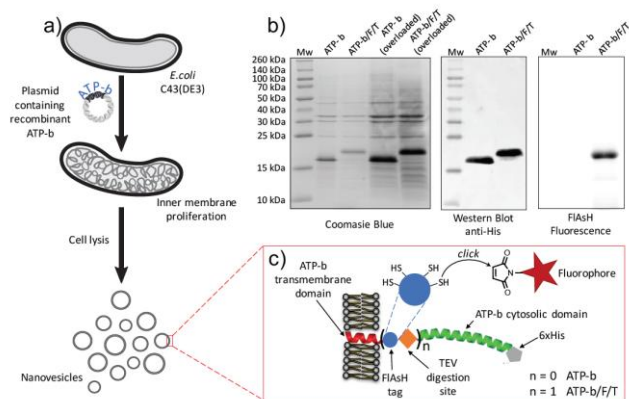


Figure 1. a) Schematic representation of the preparation of lipid:protein nanovesicles b) SDS-PAGE analysis of isolated vesicles and c) cartoon of ATP-b and ATP-b/F/T recombinant proteins. FIAsh tag contain four *clickable* thiol sites and TEV digestion site enables for post-cleavage of ATP-b cytosolic domain.

Production yield and qualitative compositions of lipid:protein membranes were determined on isolated vesicles obtained after bacterial lysis and differential centrifugation (Figure S2). Applying this straightforward and fully scalable procedure, we typically obtained 50 mg of proteins and 10 mg of lipids per liter of culture (Table S1). These amounts well above the yield of outer membrane vesicles production, which is generally around 0.5 mg of vesicles per liter of culture containing c.a. 100 µg of proteins.^[21,22] Determination of lipid composition of purified membranes indicated a mixture of phosphatidylglycerol, cardiolipin and phosphatidylethanolamine in molar percentages of 18%, 12% and 70% respectively. Purified nanovesicles exhibited an unexpectedly low lipid:protein ratio (ca. 0.2 wt/wt), showing that the overproduced proteins are densely packed in the membranes. For comparison, common formulation methods of membrane protein reconstitution into artificial liposomes work in a large excess of lipids, at lipid:protein ratios of about 10 to 800 wt/wt and require the use of detergents.^[23] The present *in vivo* bacterial bioproduction system achieves higher protein density than any reported method with no need for detergent, neither organic solvents that may denature proteins.

The isolated vesicles contained predominantly the overproduced ATP-b scaffold (Figure 1b). The bands of ATP-b (17 kDa) and ATP-b/F/T (20 kDa) were identified in SDS-PAGE by both Western Blot anti His tag and FIAsh tag *in gel* fluorescence (Figure 1b, using FIAsh-EDT₂ pro-fluorophore). In overloaded gels, Coomassie blue staining showed two additional major protein bands (Figure 1b). They were identified as OmpA (37 kDa) and OmpF (39 kDa) by MS. The three major protein components (ATP-b scaffold, OmpA and OmpF) were individually quantified using the fluorescence of tryptophan (Table S2).^[24] Target peptides (ATP-b and ATP-b/F/T) represent ca. 20% wt/wt., whereas the sum of OmpA and OmpF accounts for ca. 40% wt/wt. of all proteins. Of note, this weight percentage corresponds to a clearly dominant molar fraction of the ATP-b peptide because of its low molecular weight (Mw of ATP-b is about a tenth of OmpA and OmpF ones). Based on an estimate of total mass of all proteins (determined by bicinchoninic acid assay), the sum of other proteins (each one being present in

trace amount, see Figure 1b overloaded lanes) can be estimated to account for 40% wt/wt. The presence of OmpA and OmpF (major outer membrane proteins forming water-filled unspecific pores) in cytosolic membranes is not fully understood. It cannot be excluded that membrane proliferation may have facilitated unusual insertion of Omp or that contamination occurred during cell disruption, a point that will deserve future optimizations.

The orientation of the overproduced polypeptides in the lipidic bilayer was evaluated by assessing the accessibility of ATP-b C-terminal soluble domain to water soluble proteases.^[17,25] As trypsin do not spontaneously cross lipid bilayers, the solution-accessible domains (outer corona of proteoliposomes) are degraded much faster than inner components. Both ATP-b and ATP-b/F/T were significantly degraded after 12h of incubation at 30 °C in the presence of trypsin (< 5% of initial intensity remains) (Figure 2). When the proteoliposomes were solubilized by addition of a surfactant, further progression of trypsinolysis was observed (complete degradation of ATP-b, ATP-b/F/T, OmpA and of proteins from 40 to 100 kDa, see Figure S4 in SI). Regular progression of the proteolysis was observed in a time-course experiment (Figure S5 in SI). ATP-b/F/T were also treated with TEV protease. Specific cleavage of ATP-b/F/T soluble domain occurred at the expected position, generating a small polypeptide, which retained the fluorescence intensity of FIAsh (Figure 2). These results indicate that both the tags and cytosolic domain of ATP-b and ATP-b/F/T point towards the exterior of the nanovesicles. It should be noted that this almost 100% oriented display of custom, *clickable* polypeptides is hardly achieved in artificial formulation of liposomes.

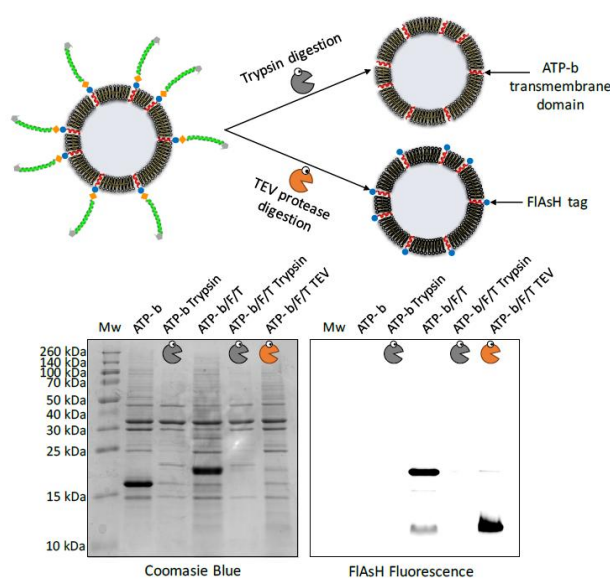


Figure 2. *In vesicle* enzymatic digestion of ATP-b and ATP-b/F/T using non-specific (trypsin) or sequence specific (TEV) proteases.

Size distribution and thiol-Michael conjugation of the nanovesicles

The size and dispersity of vesicles were first measured by DLS to explore the impact of mechanical shear used during cell lysis (Figure S3 in SI). Increasing the extrusion pressure (from 0.25 to 2 kBar) gradually decreased the vesicle mean diameter from ~200 nm to 125 nm. Polydispersity index (PDI) was also slightly decreased by application of higher pressures. 2.0 kBar was

selected as optimal lysis pressure to obtain vesicles with the narrowest possible size distribution (Table S3). Under these conditions, the diameter of nanovesicles ranged from 100 to 125 nm and PDI was < 0.2 . This size dispersity is similar to what is typically achieved by a few extrusion cycles of artificially formulated liposomes (PDI of about 0.25 compared to 0.18 in our case).^[26] Negative staining TEM images show circular objects in both ATP-b and ATP-b/F/T samples, confirming the presence of lipidic nanovesicles (Figure S6 in SI).

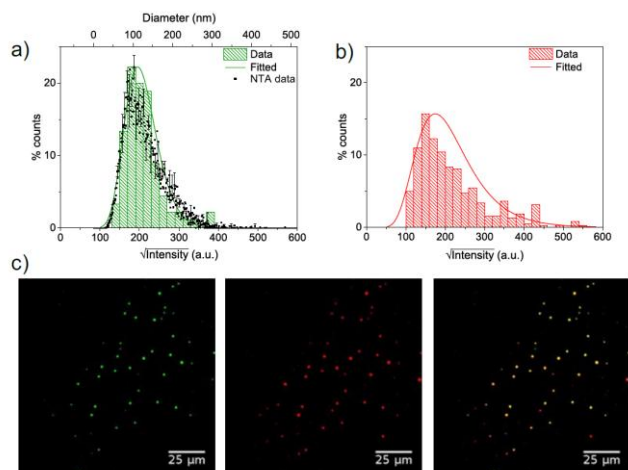
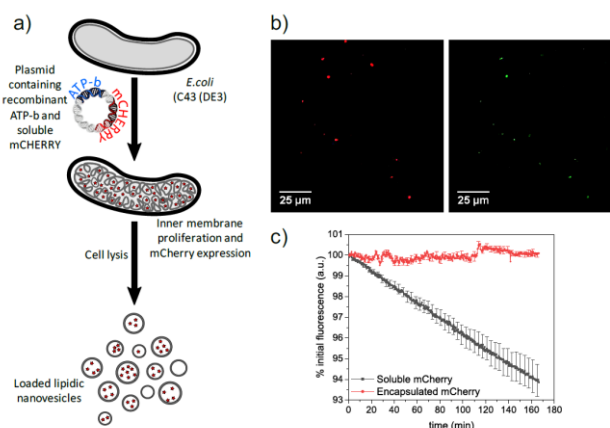


Figure 3. Size and fluorescence intensity distribution of ATP-b/F/T nanovesicles a) nonspecific lipid bilayer spDiO staining and b) Alexa-647 selective staining of ATP-b/F/T peptide. c) Fluorescence microscopy image of nanovesicles stained with spDiO (green), Alexa-647 (red) and merged images (yellow).

Next, the population of nanovesicles was characterized by single particle counting using Nanoparticle Tracking Analysis (NTA) and the microfluidic device described by Friedrich *et al.*^[27] The lipidic bilayer was nonspecifically marked using the lipophilic green fluorescent dye spDiO whereas the ATP-b peptide was stained with Alexa-647, emitting at near infrared to avoid channel cross-talk. Alexa-647 was selectively conjugated to ATP-b/F/T FIAsh moieties using thiol-maleimide *click chemistry* (Figure S7). A single and slightly shifted band compared to unstained sample was observed in SDS-PAGE gels for ATP-b/F/T after conjugation (Figure S8). These results suggest that i) the coupling reaction can be detected and ii) the vesicles could be selectively marked on ATP-b/F/T polypeptides. The fluorescence distribution curves (Figure 3a-b) allow to compare protein and lipids distributions in the vesicle population. Similarity between NTA and spDiO fluorescence intensity distributions (Figure 3a) suggests that the nonspecific spDiO dye is evenly distributed among the nanovesicle population and is a fair reporter of the lipid surface. The agreement between size-distributions measured by DLS and NTA reinforces this statement (Figure S9). ATP-b/F/T fluorescence was homogeneously distributed among the nanovesicle population in a lognormal distribution, slightly broader than the lipid one (Figure 3b). A possible explanation of broadening is the presence of a minor amount of polypeptides with low or no lipids. To assess whether lipids and proteins are colocalized or form distinct assemblies we imaged by fluorescence microscopy vesicles immobilized into Koliphor[®] hydrogels. Measurements of pixel intensity correlation^[28] (Pearsons coefficient = 0.77 ± 0.08

and Manders coefficients, $M_{\text{green}} = 0.87 \pm 0.03$ and $M_{\text{red}} = 0.82 \pm 0.02$) confirmed that most proteins are embedded in liposomes. The presence of a few particles stained in protein channel but unstained in lipid channel supports the aforementioned hypothesis of a minor fraction of protein-enriched clusters (Figure 3c).

Figure 4. a) Schematic representation of the *in vivo* production of mCherry loaded nanovesicles. b) Fluorescence microscopy image of mCherry loaded nanovesicles (mCherry in red channel and spDiO in green channel) and c)



degradation kinetic of free and encapsulated mCherry when exposed to proteases. Error bars account for relative error.

In cellulo loading

Finally, we applied this bacterial expression platform to encapsulate soluble proteins (Figure 4). Usual *in vitro* encapsulations of water soluble molecules in the interior of liposomes require conditions that may denature proteins, such as freeze-drying, the presence of detergents, or interfaces with organic solvents.^[29–31] For this reason, encapsulation of denaturation-prone enzymes or proteins remains challenging. The soluble fluorescent protein mCherry was co-expressed with ATP-b under the same T7 promoter using a single plasmid (Figure S1). Nanovesicles were isolated using the same procedure as described above. Fluorescence microscopy images of mCherry loaded nanovesicles immobilized in a Koliphor[®] hydrogel showed fluorescent dots dispersed in a dark background (Figure 4b, red channel). Colocalization with non-specific lipophilic spDiO staining revealed that most of the nanovesicles are loaded with mCherry (Figure 4b green channel and Figure S9). In addition, Western-Blot confirmed the presence of mCherry into nanovesicles (Figure S10c). Fluorescence spectra of free and nanovesicle entrapped mCherry are similar (Figure S11). Altogether, these results point to an encapsulation of native soluble mCherry inside the inner cavity of the nanovesicles. Protective properties of the lipidic nanovesicles against external environment were tested by protease digestion experiments. Fluorescence of soluble mCherry steadily decreased when non-encapsulated mCherry was mixed with proteases. In contrast, the fluorescence of mCherry-loaded nanovesicles was preserved under the same experimental conditions (Figure 4c).

Conclusions and perspectives

In summary, a robust and high yield method is proposed for the bioproduction of lipidic nanovesicles decorated with a genetically-engineered, custom polypeptide corona that can be easily (post)-modified. The density of the polypeptide corona largely exceeds (>20 fold) values achieved in artificial formulations of proteo-liposomes and enables to reach >95% orientation of C-ter end toward the outer solution. This C-ter domain remains accessible to post-modifications including *in vitro* sequence-specific cleavage and/or selective thiol-maleimide addition *click* conjugation. Furthermore, co-expressed soluble proteins can be encapsulated in the interior of the nanovesicles, as exemplified with mCherry.

The dense and almost fully oriented array of *clickable* peptides displayed on the top of vesicles could be particularly advantageous for applications requiring a high surface density functionalization (e.g. introduction of photodynamic therapy agents or macromolecules for enhanced shelf-life or vesicle-inducing fusions).^[32,33] As multiple tags can be introduced, they could allow multiple-functionalizations; for instance to combine specific targeting ligands with bio-repellent molecules.^[34] Alternatively, proteoliposomes are specially adapted as signal amplification systems in biosensors.^[35] The present method provides a mild *in vivo* encapsulation of fluorescent proteins and possibilities for a dense surface display of fluorophores that should be useful for developing probes with high brightness. Finally, reconstitution of artificial cell mimics and liposome-based sensors is often struggling for co-encapsulating soluble enzymes and membrane proteins in capsules.^[36–38] The present bioproduced lipidic vesicles offers a simple mean to combine all these constituents into well-defined assemblies.

Acknowledgements

This work was supported by CNRS, INSERM and Ecole Normale Supérieure. We acknowledge funding to support JR from the 'Initiative d'Excellence' program from the French State (Grant 'DYNAMO', ANR-11-LABEX-0011-01) and from the ANR GeneCap (ANR-17-CE09-0007).

We are grateful to Sandrine Masscheleyn for the training on proteomics (MS identification of OmpA and OmpF). We thank Dr. Audry Solgadi for lipid analysis by MS and the Région Ile de France for co-funding the SAMM MS Facility at IPSIT (Chatenay-Malabry, France)

Keywords: nanovesicle • *click* post-modification • encapsulation • bacterial production • fluorescent engineered polypeptides

- [1] J. M. Clomburg, A. M. Crumbley, R. Gonzalez, *Science* (80-.). **2017**, 355.
- [2] G. Q. Chen, *Chem. Soc. Rev.* **2009**, 38, 2434–2446.
- [3] R. Prasad, R. Pandey, I. Barman, *Wiley Interdiscip. Rev. Nanomedicine Nanobiotechnology* **2016**, 8, 316–330.
- [4] J. Palomo, M. Filice, *Nanomaterials* **2016**, 6, 84.
- [5] N. M. Matsumoto, P. Prabhakaran, L. H. Rome, H. D. Maynard, *ACS Nano* **2013**, 7, 867–874.
- [6] W. F. Rurup, J. Snijder, M. S. T. Koay, A. J. R. Heck, J. J. L. M. Cornelissen, *J. Am. Chem. Soc.* **2014**, 136, 3828–3832.
- [7] P. da Silva Malheiros, D. J. Daroit, A. Brandelli, *Trends Food Sci. Technol.* **2010**, 21, 284–292.
- [8] A. Etemadi, M. Kouhi, S. Alimirzalu, A. Akbarzadeh, *Artif. Cells, Nanomedicine, Biotechnol.* **2016**, 44, 381–391.
- [9] E. V. Batrakova, M. S. Kim, *J. Control. Release* **2015**, 219, 396–405.
- [10] J. P. K. Armstrong, M. N. Holme, M. M. Stevens, *ACS Nano* **2017**, 11, 69–83.
- [11] G. Fuhrmann, A. Serio, M. Mazo, R. Nair, M. M. Stevens, *J. Control. Release* **2015**, 205, 35–44.
- [12] J. P. Frohnmayer, D. Brüggemann, C. Eberhard, S. Neubauer, C. Mollenhauer, H. Boehm, H. Kessler, B. Geiger, J. P. Spatz, *Angew. Chemie - Int. Ed.* **2015**, 54, 12472–12478.
- [13] C. M. Cole, R. J. Brea, Y. H. Kim, M. D. Hardy, J. Yang, N. K. Devaraj, *Angew. Chemie - Int. Ed.* **2015**, 54, 12738–12742.
- [14] F. Farjadian, M. Moghoofei, S. Mirkiani, A. Ghasemi, N. Rabiee, S. Hadifar, A. Beyzavi, M. Karimi, M. R. Hamblin, *Biotechnol. Adv.* **2018**, 36, 968–985.
- [15] M. J. H. Gerritzen, D. E. Martens, R. H. Wijffels, L. van der Pol, M. Stork, *Biotechnol. Adv.* **2017**, 35, 565–574.
- [16] H. M. Eriksson, P. Wessman, C. Ge, K. Edwards, Å. Wieslander, *J. Biol. Chem.* **2009**, 284, 33904–33914.
- [17] I. Arechaga, B. Miroux, S. Karrasch, R. Huijbregts, B. De Kruijff, M. J. Runswick, J. E. Walker, *FEBS Lett.* **2000**, 482, 215–219.
- [18] B. Miroux, J. E. Walker, *J. Mol. Biol.* **1996**, 260, 289–298.
- [19] G. Carranza, F. Angius, O. Illoia, A. Solgadi, B. Miroux, I. Arechaga, *Biochim. Biophys. Acta - Biomembr.* **2017**, 1859, 1124–1132.
- [20] S. R. Adams, R. E. Campbell, L. A. Gross, B. R. Martin, G. K. Walkup, Y. Yao, O. Juan Llopis, R. Y. Tsien*, *Jacs* **2002**, 6063–6076.
- [21] O. Y. Kim, B. S. Hong, K.-S. Park, Y. J. Yoon, S. J. Choi, W. H. Lee, T.-Y. Roh, Y.-K. Kim, Y. S. Gho, *Bio-protocol* **2013**, 3, e995.
- [22] W. D. McCaig, A. Koller, D. G. Thanassi, *J. Bacteriol.* **2013**, 195, 1120–1132.
- [23] J. L. Rigaud, B. Pitard, D. Levy, *BBA - Bioenerg.* **1995**, 1231, 223–246.
- [24] W. Holzmüller, U. Kulozik, *J. Food Compos. Anal.* **2016**, 48, 128–134.
- [25] J.-L. Rigaud, D. B. T.-M. in E. Lévy, in *Liposomes, Part B*, Academic Press, **2003**, pp. 65–86.
- [26] B. J. Frisken, C. Asman, P. J. Patty, *Langmuir* **2000**, 16, 928–933.
- [27] R. Friedrich, S. Block, M. Alizadehheidari, S. Heider, J. Fritzsche, E. K. Esbjörner, F. Westerlund, M. Bally, *Lab Chip* **2017**, 17, 830–841.
- [28] K. W. Dunn, M. M. Kamocka, J. H. McDonald, *Am. J. Physiol. Physiol.* **2011**, 300, C723–C742.
- [29] T. M. Allen, P. R. Cullis, *Adv. Drug Deliv. Rev.* **2013**, 65, 36–48.
- [30] J. Gubernator, *Expert Opin. Drug Deliv.* **2011**, 8, 565–580.
- [31] D. Zucker, D. Marcus, Y. Barenholz, A. Goldblum, *J. Control. Release* **2009**, 139, 73–80.
- [32] X. Cai, D. Mao, C. Wang, D. Kong, X. Cheng, B. Liu, *Angew. Chemie - Int. Ed.* **2018**, 211816, 16396–16400.
- [33] W. Xu, J. Wang, J. E. Rothman, F. Pincet, *Angew. Chemie - Int. Ed.* **2015**, 54, 14388–14392.
- [34] T. Curk, J. Dobnikar, D. Frenkel, *Proc. Natl. Acad. Sci.* **2017**, 114, 7210 LP-7215.
- [35] Q. Liu, B. J. Boyd, *Analyst* **2013**, 138, 391–409.

- [36] M. Yoshimoto, S. Wang, K. Fukunaga, D. Fournier, P. Walde, R. Kuboi, K. Nakao, *Biotechnol. Bioeng.* **2005**, *90*, 231–238.
- [37] V. Vamvakaki, D. Fournier, N. A. Chaniotakis, *Biosens. Bioelectron.* **2005**, *21*, 384–388.
- [38] V. Vamvakaki, N. A. Chaniotakis, *Biosens. Bioelectron.* **2007**, *22*, 2848–2853.

